Evaluation of mixed-mode stress intensity factor of wood from crack-tip displacement fields utilizing digital image correlation

JIAN ZHAO
School of Technology
Beijing Forestry University
Tsinghua East Street 35, Haidian, Beijing, China
CHINA
zhaojian1987@bjfu.edu.cn
DONG ZHAO
School of Technology
Beijing Forestry University
Tsinghua East Street 35, Haidian, Beijing, China
CHINA
zhaodong68@bjfu.edu.cn

Abstract: - The effects of anisotropy and varying initial crack angle during mixed mode tension loading were studied in Dahurian Larch wood. The mixed mode stress intensity factors (SIFs), K_I and K_{II}, were calculated using displacements from digital image correlation. With the crack angle increasing, the SIF of mode I in unilateral crack increase all along, but the SIF of mode II in unilateral crack shows an initial increase, followed by a decrease. Crack-tip plastic zones were determined using an anisotropic yield criterion. Strains in the plastic zone obtained from digital image correlation showed that the varying angles of crack growth have on the asymmetry of the plastic zone. Experimental results reveal that the DIC method is a practical and effective technique for SIF and crack-tip plastic size measurement.

Key-Words: - Digital image correlation, Stress intensity factor, Mixed mode, Crack-tip plastic zone

1 Introduction

Wood is probably the most ancient engineering materials in the world. Although many new structural materials and composite materials are emerging continuously, wood is still widely used today in many species for all kinds of purposes. Its application in modern engineering structures of large dimensions like stadium roofs and floors or long-span bridges calls for a good understanding of mechanical properties, one important aspect of which is the resistance to fracture. Structural wood members contain natural or artificial defects such as knots, holes, splits, and machined notches that cause stress concentration within the material [1]. According to linear elastic fracture mechanics [2], the behavior of a crack in material can be characterized completely by the stress intensity factor (SIF) which reflects the effect of loading, crack size and crack shape. Also, the displacement field, the stress field and strain field near the crack tip can be characterized by SIF.

In wood, there are six principal systems of crack propagation for the three orthotropic planes (Radial (R), Tangential (T) and longitudinal (L)) can be defined as LR, LT, TL, RL, RT, and TR. The first letter indicates the normal to the crack plane and the second letter describes the direction of crack propagation. In practice, cracks never propagate in the LR or LT direction because that would require fracture of the wood fibers. Instead, cracks orient in those direction turn to become RL, TL, RT, or TR fracture [3]. In order to use fracture mechanics in wood structures, the fracture behaviour of wood has to be known. At present, relatively little is known about the fracture phenomena in wood and, in particular, the displacement field ahead of the crack tip and the plastic zone around the crack tip. Fracture mechanics research has used optical techniques as a method to characterize near tip displacement and stress fields in the recent past such as photoelasticity [4], moiré interferometry [5], contact caustics [6], and digital image correlation (DIC) [7]. Due to its simplicity and effectiveness, recently, DIC as one kind of optical methods has been used to study fracture parameters for a cracked body. Samarasinghe [8, 9] used DIC to obtain full field surface displacement measurements in wood specimens and investigated displacement fields near to the crack tip. They concluded that the DIC technique is useful for the detailed analysis of displacements and SIF in wood. However, they did not to investigate the conditions near the crack tip and ensuing plastic region and its size.

A crack represents a singular point of stress concentration within the wood and introduces localized plasticity ahead of the crack tip. In the case of an isotropic body under pure mode I loading, the plastic zone has been observed to be symmetric. In the case of combined mode I and mode II loading in an anisotropic body, the plastic zone is asymmetric. Absolute majority cracks consist in structural wood members are inclined cracks. Inclined cracks can experience mixed mode crack growth. The angle of this inclination has also been shown to have an effect on the plastic zone shape [10, 11]. The stress intensity factors, K_I and K_{II}, can be used to describe the size and shape of the plastic zone [12, 13].

This study gives insight into mixed-mode stress intensity factor of wood, the effect of the angle of inclination of the crack plane on the stress intensity factor and the shape of the plastic zone around the crack tip. Displacements obtained from digital image correlation method were used to determine the stress intensity factors and to characterize the plastic zone ahead of the crack tip. The first section of this paper discusses the basic concepts of DIC method and extracts the crack tip displacement field information from the DIC results and the calculations of the plastic zone size and shape. The second section discusses the materials and equipment employed for the experimental testing. As mixed mode stress intensity factors can be evaluated simply and by digital image correlation, it is expected that the proposed method can be applied to various fracture problems during experimental evaluation of structural components.

2 Methods

2.1 Theory of Digital Image Correlation

As an advance photomechanics method, Digital Image Correlation (DIC) has proven to be an effective and useful tool for deformation analysis in the field of experimental solid mechanics [14, 15]. DIC technique is a non-contact optical measurement method used to obtain full-field displacements of an object surface through monitoring and measuring deformations on an object surface as it undergoes loading. This technique starts with getting the specimen surface image before loading (reference image), and then a series of images are taken during the deformation process (current images). The surface of the specimen has a random gray speckle pattern applied to it. All the deformed images show a different random speckle pattern relative to the initial undeformed reference image. DIC compares the gray scale of a chosen subset in undeformed and deformed images to evaluate deformation. The analysis procedure of the DIC method is shown in Fig. 1.

Let us consider f the image of the reference configuration and its corresponding current image g after deformation. The gray level conservation at any pixel location x then reads [16]

$$f(\mathrm{x}) = g\big(\mathrm{x} + \mathbf{u}(\mathrm{x})\big) \tag{1}$$

where $\mathbf{u}$ is the displacement function. Calculating the grayscale correlation coefficient will lead to finding the corresponding relationship between reference and current images for establishing the displacements of subset. The correlation coefficient ρ is calculated by

$$\rho = \int_{\Omega} [f(\mathrm{x}) - g(\mathrm{x} + \mathbf{u}(\mathrm{x}))]^2 d\mathrm{x} \tag{2}$$

Minimization of the above correlation coefficient would provide the best estimate of the desired displacements. Thus we have

$$\frac{\partial \rho}{\partial(\mathbf{u}(\mathrm{x}))} = 0 \tag{3}$$

Newton-Raphson iteration method is used to solve the above nonlinear equation.

2.2 Crack-tip displacement & strain fields and plastic zone analysis

For mode I and mode II mixed mode crack problems, the crack tip displacements for an orthotropic body loaded in tension are expressed as [17,18]

$$u = K_I \sqrt{\frac{2r}{\pi}} \mathrm{Re}\left[\frac{1}{\mu_1 - \mu_2}\left(\mu_1 p_2 \sqrt{\cos\theta + \mu_2 \sin\theta} - \mu_2 p_1 \sqrt{\cos\theta + \mu_1 \sin\theta}\right)\right] + K_{II} \sqrt{\frac{2r}{\pi}}$$

$$\times \operatorname{Re}\left[\frac{1}{\mu_1-\mu_2}\left(p_2\sqrt{\cos\theta+\mu_2\sin\theta}-p_1\sqrt{\cos\theta+\mu_1\sin\theta}\right)\right]+a_{11}Tr\cos\theta+Ar\sin\theta+B_u \quad (4)$$

$$v=K_I\sqrt{\frac{2r}{\pi}}\operatorname{Re}\left[\frac{1}{\mu_1-\mu_2}\left(\mu_1 q_2\sqrt{\cos\theta+\mu_2\sin\theta}-\mu_2 q_1\sqrt{\cos\theta+\mu_1\sin\theta}\right)\right]+K_{II}\sqrt{\frac{2r}{\pi}}$$
$$\times \operatorname{Re}\left[\frac{1}{\mu_1-\mu_2}\left(q_2\sqrt{\cos\theta+\mu_2\sin\theta}-q_1\sqrt{\cos\theta+\mu_1\sin\theta}\right)\right]+a_{12}Tr\sin\theta+Ar\cos\theta+B_v \quad (5)$$

where Re denotes the real part of a complex number.

$$p_j=a_{11}\mu_j^2+a_{12} \quad (6)$$
$$q_j=a_{12}\mu_j+\frac{a_{22}}{\mu_j} \quad (7)$$

K_I and K_{II} are the mode I and mode II stress intensity factors respectively, T is the T-stress, A is the rigid body rotation, B_u and B_v are the rigid body translations in the u and v directions respectively, r and θ are the polar coordinates with the origin at the crack tip, μ_1 and μ_2 are the roots from the following characteristic Eq. (8), and a_{ij} are the elastic constants and can be classically expressed in the orthotropic base (L,T) with Voigt notations $\boldsymbol{a}=\begin{bmatrix}a_{11} & a_{12} & 0\\ a_{21} & a_{22} & 0\\ 0 & 0 & a_{66}\end{bmatrix}=\begin{bmatrix}1/E_L & -\nu_{LT}/E_L & 0\\ -\nu_{TL}/E_T & 1/E_T & 0\\ 0 & 0 & 1/G_{LT}\end{bmatrix}_{(L,T)}$ with symmetry, positiveness and definiteness conditions. E_α are Young's modulus in direction $\alpha=L,T$, $\nu_{\alpha\beta}$ are Poisson coefficients, $G_{\alpha\beta}$ are the shear modulus. These two μ's are the two complex conjugate roots for which the imaginary parts are positive.

$$a_{11}\mu^4+(2a_{12}+a_{66})\mu^2+a_{22}=0 \quad (8)$$

With the stress intensity factors for mode I and mode II known, the stress field, Eq. (9), around the crack tip was determined. The stress field was used to determine the plastic zone size and shape. The stresses are

$$\left.\begin{aligned}\sigma_x&=\frac{K_I}{\sqrt{2\pi r}}(F_{Ix}+mF_{IIx})\\ \sigma_y&=\frac{K_I}{\sqrt{2\pi r}}(F_{Iy}+mF_{IIy})\\ \tau_{xy}&=\frac{K_I}{\sqrt{2\pi r}}(F_{Ixy}+mF_{IIxy})\end{aligned}\right\} \quad (9)$$

where $m=K_{II}/K_I$ and the F terms in Eq. (9) are expressed as

$$\left.\begin{aligned}F_{Ix}&=\operatorname{Re}\left[\frac{\mu_1\mu_2}{\mu_1-\mu_2}\left(\frac{\mu_2}{\sqrt{\cos\theta+\mu_2\sin\theta}}-\frac{\mu_1}{\sqrt{\cos\theta+\mu_1\sin\theta}}\right)\right]\\ F_{Iy}&=\operatorname{Re}\left[\frac{1}{\mu_1-\mu_2}\left(\frac{\mu_1}{\sqrt{\cos\theta+\mu_2\sin\theta}}-\frac{\mu_2}{\sqrt{\cos\theta+\mu_1\sin\theta}}\right)\right]\\ F_{Ixy}&=\operatorname{Re}\left[\frac{\mu_1\mu_2}{\mu_1-\mu_2}\left(\frac{1}{\sqrt{\cos\theta+\mu_1\sin\theta}}-\frac{1}{\sqrt{\cos\theta+\mu_2\sin\theta}}\right)\right]\end{aligned}\right\} \quad (10)$$

$$\left.\begin{aligned}F_{IIx}&=\operatorname{Re}\left[\frac{1}{\mu_1-\mu_2}\left(\frac{\mu_2^2}{\sqrt{\cos\theta+\mu_2\sin\theta}}-\frac{\mu_1^2}{\sqrt{\cos\theta+\mu_1\sin\theta}}\right)\right]\\ F_{IIy}&=\operatorname{Re}\left[\frac{1}{\mu_1-\mu_2}\left(\frac{1}{\sqrt{\cos\theta+\mu_2\sin\theta}}-\frac{1}{\sqrt{\cos\theta+\mu_1\sin\theta}}\right)\right]\\ F_{IIxy}&=\operatorname{Re}\left[\frac{1}{\mu_1-\mu_2}\left(\frac{\mu_1}{\sqrt{\cos\theta+\mu_1\sin\theta}}-\frac{\mu_2}{\sqrt{\cos\theta+\mu_2\sin\theta}}\right)\right]\end{aligned}\right\} \quad (11)$$

Since the wood exhibits anisotropic properties, Hill's extension of the von Mises's yield criterion was used [19]. The yield criterion in quadratic form is expressed as

$$E(\sigma_y-\sigma_z)^2+G(\sigma_x-\sigma_z)^2+H(\sigma_x-\sigma_y)^2$$
$$+2L\tau_{yz}^2+2M\tau_{xz}^2+2N\tau_{xy}^2=1 \quad (12)$$

$$\left.\begin{aligned}2E&=-\frac{1}{X^2}+\frac{1}{Y^2}+\frac{1}{Z^2}\\ 2G&=\frac{1}{X^2}-\frac{1}{Y^2}+\frac{1}{Z^2}\\ 2H&=\frac{1}{X^2}+\frac{1}{Y^2}-\frac{1}{Z^2}\\ 2N&=\frac{1}{S^2}\end{aligned}\right\} \quad (13)$$

where E, G, and H are coefficients that characterize the anisotropy in the normal directions and L, M, and N are the coefficients that characterize the shear anisotropy. X, Y, and Z are the yield stresses in the principal directions and S is the shear yield stress. Assuming plane stress since the specimens are thin, $\sigma_z=\sigma_{xz}=\sigma_{yz}$ and Eq. (12) reduces to

$$(G+H)\sigma_x^2-2H\sigma_x\sigma_y+(E+H)\sigma_y^2+2N\tau_{xy}^2=1 \quad (14)$$

To find the plastic zone size, we substituted Eq. (9) into Eq. (14) and solved for the plastic zone radius, r_p, with the final form [20]:

$$r_p=\frac{K_I^2}{2\pi}\left\{\begin{aligned}&(G+H)(F_{Ix}+mF_{IIx})^2-2H(F_{Ix}+mF_{IIx})(F_{Iy}+mF_{IIy})\\ &+(E+H)(F_{Iy}+mF_{IIy})^2+2N(F_{Ixy}+mF_{IIxy})^2\end{aligned}\right\} \quad (15)$$

2.3 Crack-tip localization algorithm

Calculating and analyzing the stress intensity factors and the plastic zone size needs firstly to localize the crack tip. Opening crack will cause geometric discontinuities in the cross section. Here, a method based on digital image correlation is used in order to localize discontinuities even if the end of the crack is not visible [21]. Two points P and Q are considered in the reference image (Fig.2). Then, a displacement field, $\mathbf{u}(x)$, is applied in such a way that the corresponding points in the current image (P' and Q') are separated by a crack.

A measurement of the discontinuity between the two points P and Q is denoted $P ₪ Q$ and defined in Eq. (16).

$$P ₪ Q = \left\|\overrightarrow{P'Q'} - \overrightarrow{PQ}\right\| \tag{16}$$

Since $\forall(\mathrm{P},\mathrm{P}')$, $\overrightarrow{\mathrm{O'P'}} = \overrightarrow{\mathrm{OP}} + \mathbf{u}(\mathrm{P})$, the expression of the discontinuity between two points is rewritten in Eq. (17).

$$P ₪ Q = \|\mathbf{u}(P) - \mathbf{u}(Q)\| \tag{17}$$

where $\mathbf{u}(x)$ is still given by the minimization of Eq. (3).

From the definition of the discontinuity between two points (Eq. (16)), a criterion of discontinuity in a subset is given in Eq. (18).

$$K = \max(M ₪ N; Q ₪ P) = \max(\|\mathbf{u}(N) - \mathbf{u}(M)\|; \|\mathbf{u}(P) - \mathbf{u}(Q)\|) \tag{18}$$

This criterion of discontinuity is available if the elongations stay lower than the displacements due to the discontinuity.

2.4 Experimental material and experimental procedures

2.4.1 Specimen and material property

To demonstrate proposed technique for stress intensity factor measurement, four edge notched dog-bone specimens of Dahurian Larch wood were used in uniaxial tensile test (Fig.3). Specimens were created from a single section of a Dahurian Larch log that had been exposed to normal air since being felled. The final dog-bone shape (Fig.3) was created with a router and aluminum template. This shape has a central gage length of 60mm where the cross-section is 15mm × 4mm. The crack was sharpened with different angles of the inclination using a special knife prepared for the purpose to simulate a natural crack. All specimens were clear and straight-grained with no obvious defects.

Longitudinal modulus E_L, transverse modulus E_T, shear modulus G_{LT} and Poisson's ratio ν_{LT} were measured by electrical strain gauges using the method mentioned in Ref.[22]. The elastic properties of the Dahurian Larch wood are given in Table 1. It has been especially emphasized that all the samples were prepared from the same log mentioned above.

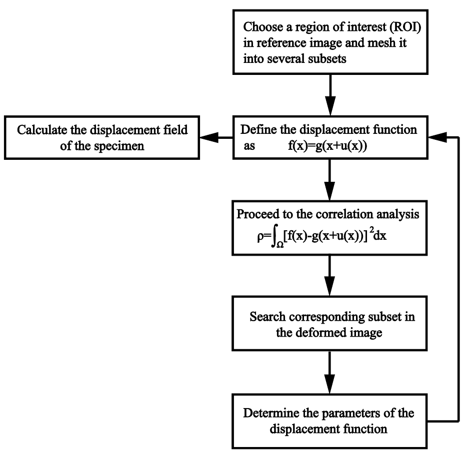

Fig. 1 Analysis procedure of digital image correlation method.

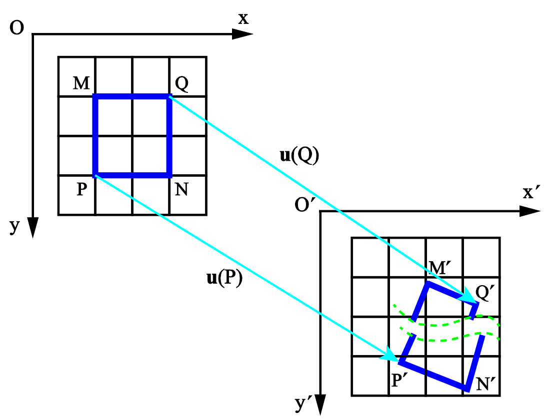

Fig. 2 Discontinuity between two points M and N caused by crack

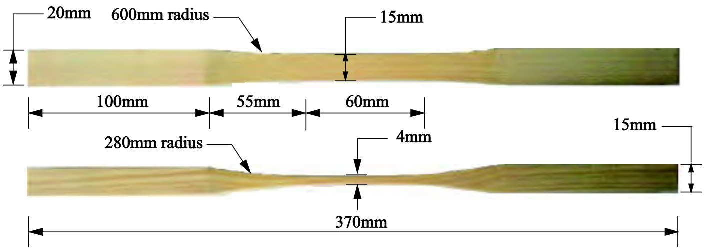

Fig. 3 Specimen configuration

Table 1. Elastic properties of Dahurian Larch

Longitudinal modulus $\boldsymbol{E_L}$ (MPa)	Transverse modulus $\boldsymbol{E_T}$ (MPa)	Shear modulus $\boldsymbol{G_{LT}}$ (MPa)	Poisson's ratio $\boldsymbol{\nu_{LT}}$
15753	696	506	0.53

2.4.2 Experimental procedures

The first step to applying the DIC method requires that the surface of the specimen must exhibit a random speckle pattern. As stated previously, the random speckle pattern allows the software to accurately determine the location of each pixel subset in the deformed images. Specimen surface preparation is accomplished by spraying the surface with white and black spray paint until a sufficient color variation exists. The bell-shaped grayscale intensity (Fig. 4) histogram distribution shows good quality of the speckle pattern which is related to the accuracy of DIC method [23].

Preparation of the testing equipment occurs after the speckle pattern application to produce a testing configuration as shown in Fig.5. Specimens were conducted in an electronically controlled single-axis Universal Materials Testing Machine. Wedge action grips were employed, which prevent the rotation of the specimen ends. One of the grips remains fixed while the other is displaced at a constant speed until specimen failure. Stress intensity factor measurement by the DIC method uses the following procedures. First, a high intensity LED light source is placed near the specimen to remove any shadows present on the specimen. Second, the CMOS camera is placed perpendicular to the surface of the specimen and at a distance which optimizes the camera focus. The CMOS camera used in this study has a resolution of 1280 x 1024 pixels. Prior to testing, a graph paper was placed against the specimen surface and its image was captured to calibrate the image distances to real distances. A typical resolution for the test set-up was 0.04549 mm/pixel. Finally, the loading was elevated to 4000 N at intervals of 100 N with the loading velocity of 0.2 mm/min and deformed images were taken at each load step. All the tests were performed in the laboratory temperature and moisture conditions (approximately 55% RH and 20°C).

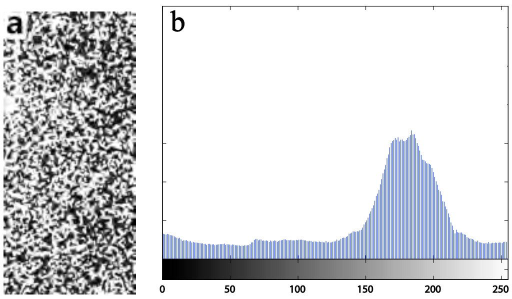

Fig. 4 The speckle pattern of the specimen surface (a) and its histogram (b)

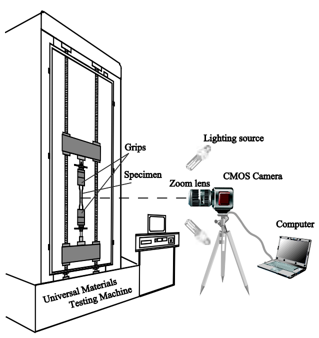

Fig. 5 Digital Image Correlation Testing Setup

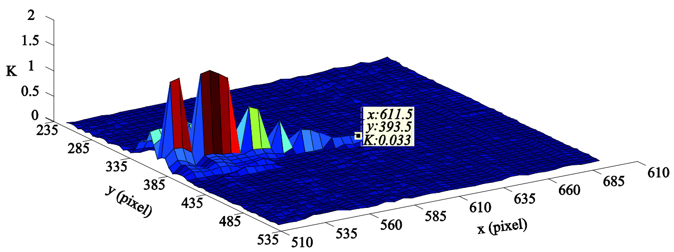

Fig. 6 Result of the crack localization

3 *Results and discussion*

3.1 Implementation of Crack-tip localization

The reference image and the deformed image under 3800N are captured and the subset size is chosen (5 × 5 pixels). Then, the criterion of discontinuity in a subset (Eq. (18)) is evaluated all over the image as shown in Figure 6. The crack position can be localized in the sub-pixel scale and the tip position is $((x_{tip}, y_{tip}) = (611.5,393.5))$.

3.2 The stress intensity factor determination in the experiments

The calculation solves for K_I and K_{II} required the crack tip displacements at a certain stage of the load process using Eqs. (4) and (5). The experimentally obtained stress intensity factors have been plotted in Figs. 7-9.

When the calculation was performed on the specimen No.1 with a horizontal crack length of 2mm and width of 0.5mm at the load of 4100N, orthotropic compliance coefficients were used in Eq. (8). Since the crack was horizontal with no shear component, there was no mode II component, and thus the mode II stress intensity factor was again nearly zero. The horizontal displacements are symmetric in Fig. 7a. The mode I stress intensity factor distribution fields for the Dahurian Larch No.1 specimen are given in Fig. 7b.

Two specimens with different initial inclined crack orientations were tested to investigate mixed mode. The No.2 specimen with the same crack size of No.1 at the load of 3800N was tested as a comparison to the specimen. The crack angle is 22.5° along the horizontal direction. The horizontal displacements are asymmetric in Fig. 8a indicating shearing or mode II displacement is occurring during the loading process. The mode I and II stress intensity factor contours are displayed in Fig. 8b and c respectively.

A second test was conducted with No.3 specimen at the load of 4670N. The crack angle is 60° along the horizontal direction. The horizontal and vertical displacements with crack length of 2 mm are displayed in Fig. 9a and b respectively. The mode I stress intensity factor contours and the mode II stress intensity factor contours are displayed in Fig. 9c and d. From above stress intensity factor contours, with the crack angle increasing, the SIF of mode I in unilateral crack increase all along, but the SIF of mode II in unilateral crack shows an initial increase, followed by a decrease.

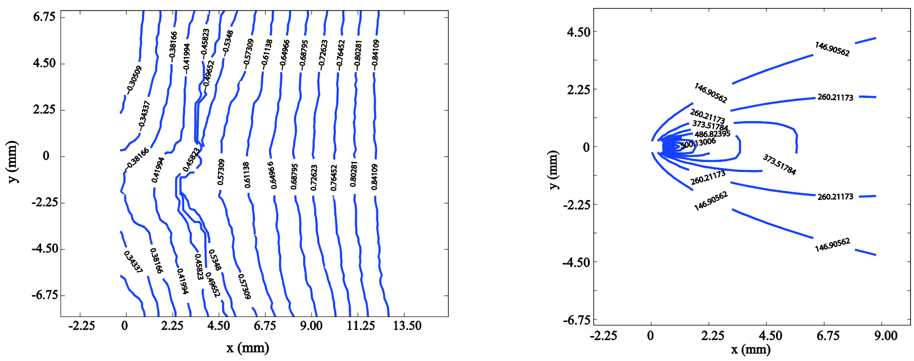

(a) (b)

Fig. 7 (a) Experimentally measured horizontal displacement contours in micrometers for specimen No.1. (b) The mode I stress intensity factor distribution fields for the Dahurian Larch No.1 specimen. The unit of SIF is $\mathrm{kN/m^{3/2}}$

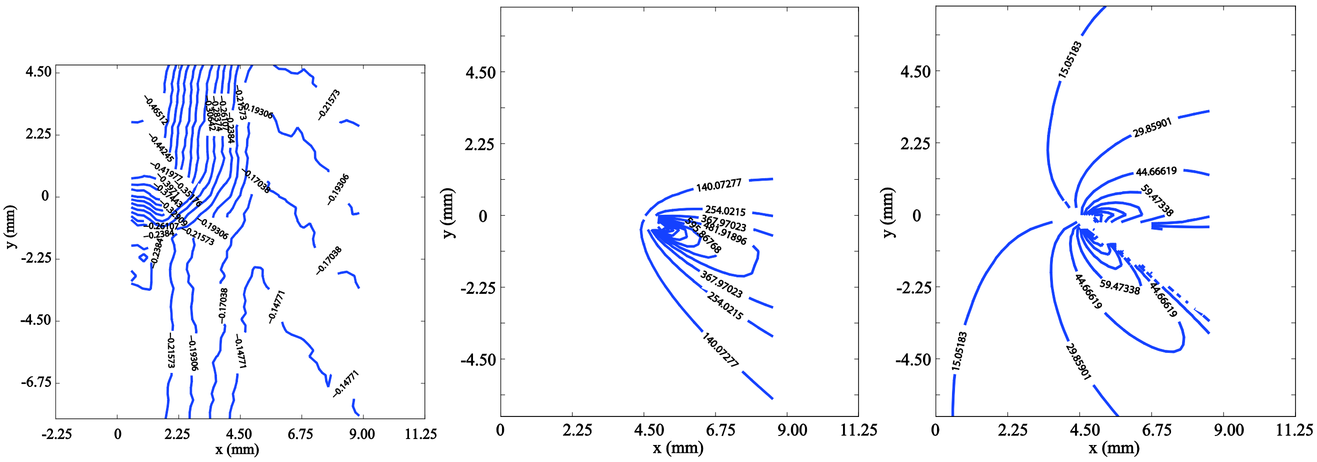

(a) (b) (c)

Fig. 8 (a) Experimentally measured horizontal displacement contours in micrometers for specimen No.2. (b) The mode I stress intensity factor distribution fields for specimen No.2. (c) The mode II stress intensity factor distribution fields for specimen No.2. The unit of SIF is $\mathrm{kN/m^{3/2}}$.

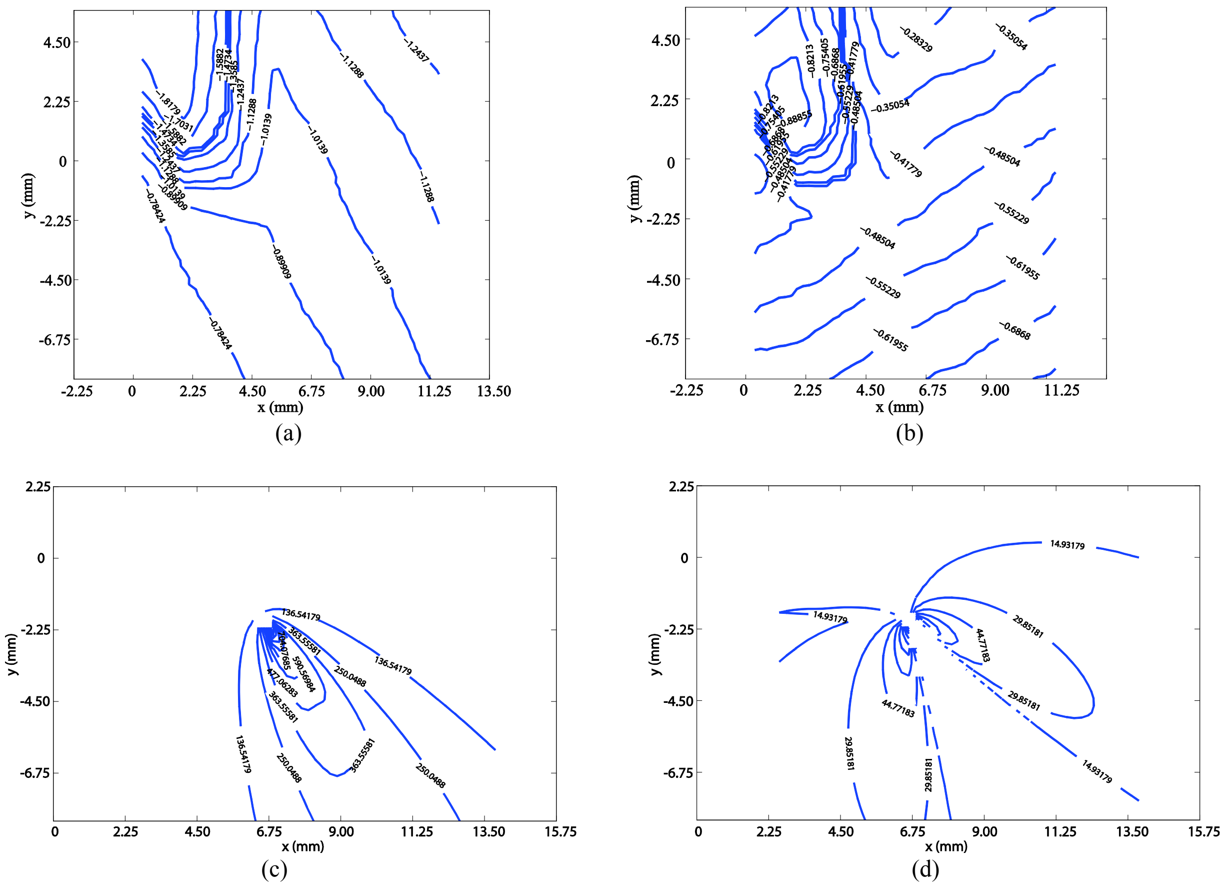

Fig. 9 Experimentally measured (a) horizontal and (b) vertical displacement contours in micrometers for specimen No.3. The (c) mode I and (d) mode II stress intensity factor distribution fields for specimen No.3. The unit of SIF is $\mathrm{kN/m^{3/2}}$

3.3 Plastic zone size

Since each image captured represents a different load throughout the loading progress, the entire progression of stresses and strains was recorded. Using Eq. (15), the plastic zone size was determined using the stress intensity factors found in the experimental analysis and the development of the size and shape throughout the loading progress was observed. DIC was used to find the strains in front of the crack tip, and the strains inside the plastic zone are shown in Fig. 10 (a-c) for 70% of the maximum load of a loading progress for each specimen tested during this study.

In the pure mode I case, the Dahurian Larch wood specimen still has a symmetric plastic zone as shown in Fig. 10 (a) at 70% of the load, the plastic zone area is $1.375mm^2$ and the DIC strains show a compact concentration. The K_{II} component in the other two specimens caused the plastic zone shape to be asymmetric. In the No.2 specimen, the plastic zone shape was shown in Fig. 10 (b). The plastic zone is larger above the crack tip, which is consistent with the displacements that were greater above the crack. The plastic zone area progression was similar to that of No.1 specimen and the plastic area at 70% of the load found was 1.523mm^2. In the No.3 specimen, the plastic zone had a shape similar to the No.2 specimen and the plastic zone size was the largest found in this study, as displayed in Fig. 10 (c). At 70% of the load, the area was 1.930mm^2.

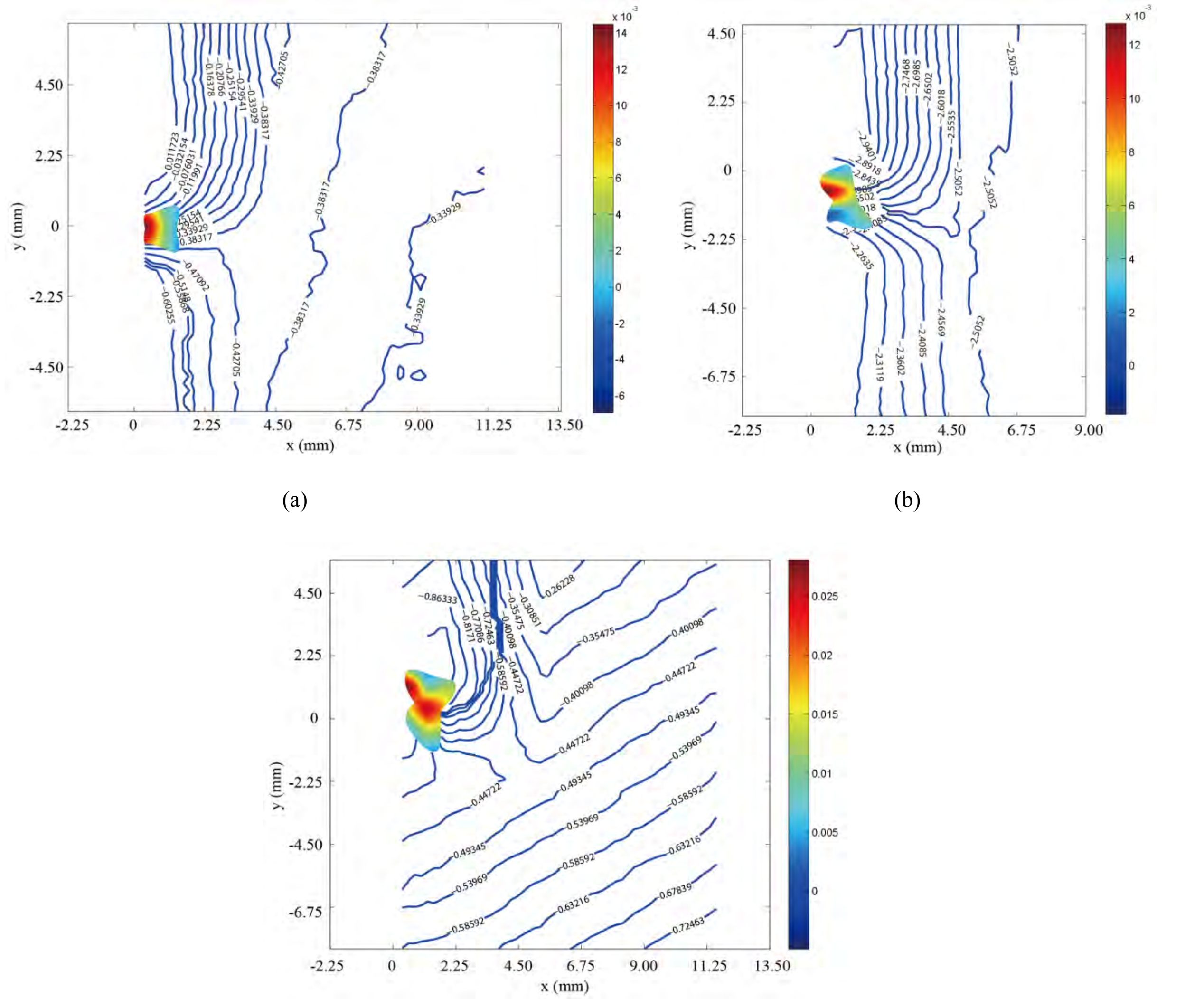

(a) (b)

(c)

Fig. 10 (a) Plastic zones and vertical displacement contours in micrometers associated with No.1 specimen, 70% load level of the maximum load with a plastic zone area of 1.375mm^2. Due to the anisotropy of the specimen, the plastic zone, with DIC strains shown inside, has an irregular shape but is still symmetric due the specimen experiencing pure mode I loading conditions. (b) Plastic zones and vertical displacement contours in micrometers associated with No.2 specimen, 70% load level of the maximum load with a plastic zone area of 1.523mm^2. The plastic zone size and DIC strains within are asymmetric due to the specimen being under mixed mode loading conditions. (c) Plastic zones and vertical displacement contours in micrometers associated with No.3 specimen, 70% load level of the maximum load with a plastic zone area of 1.930mm^2. Asymmetry in the plastic zone and DIC strains is observed due to the mixed mode loading.

4 Summary

The stress intensity factors, K_I and K_{II}, at the crack tip of the anisotropic Dahurian Larch wood specimens, which were under uniaxial tension, were determined using full field DIC displacements. With the crack angle increasing, the SIF of mode I in unilateral crack increase all along, but the SIF of mode II in unilateral crack shows an initial increase, followed by a decrease. The utilization of digital image correlation also provides for the strains around the crack tip. The plastic zone was determined using the stress field associated with the K_I and K_{II} values obtained from the experimental analysis, and the development of the strain field inside the plastic zone was observed.

By observing and analyzing the plastic zone, further insight can be gained on how anisotropy affects the plasticity ahead of a crack tip. When studying mixed mode cases, the effects that varying angles of crack growth have on the asymmetry of the plastic zone and strain development can be determined.

5 Conclusions

The main contribution of this work is the analysis of mixed-mode stress intensity factor of Dahurian Larch, the effect of the angle of inclination of the crack plane on the stress intensity factor and the shape of the plastic zone around the crack tip.

The displacement fields in the vicinity of the crack-tip of edge-cracked specimen of Dahurian Larch subjected to the tension loading of modes I and II was measured by the DIC technique.

(1) The mixed mode stress intensity factors fields were determined using displacements found from digital image correlation.
(2) The plastic zone size and shape, and the associated strain fields were found for loading progress of anisotropic specimens with the varying angles of crack.

References:

[1] S. Samarasinghe, G.D. Kulasiri, Stress intensity factor of wood from crack-tip displacement fields obtained from digital image processing, *Silva Fennica,* Vol. 38, No. 3, 2004,pp. 267-278.
[2] T.L. Anderson, *Fracture Mechanics: Fundamentals and Applications*, CRC Press, Taylor & Francis Group, 2005.
[3] I. Smith, E. Landis, M. Gong, *Fracture and Fatigue in Wood*, John Wiley & Sons, 2003.
[4] R.J. Sanford, Determining fracture parameters with full-field optical methods, *Experimental Mechanics,* Vol. 29, No. 3, 1989, pp. 241-247.
[5] C.R. Schultheisz, R.D. Pfaff, W.G. Knauss, An experimental/analytical comparison of three dimensional deformations at the tip of a crack in a plastically deforming plate, *International Journal of Fracture,* Vol. 90, No.1-2, 1998, pp. 1-25.
[6] A. Bakić, D. Semenski, S. Jecić, Contact caustics measurements expanded to anisotropic materials, *Archives of Civil and Mechanical Engineering,* Vol. XI, No. 3, 2011,pp. 497-505.
[7] S.R. McNeill, W.H. Peters, M.A. Sutton, Estimation of Stress Intensity Factor by Digital Image Correlation, *Engineering Fracture Mechanics*, Vol. 28, No. 1, 1987, pp. 101-112.
[8] S. Samarasinghe, G. D. Kulasiri, Displacement Fields of Wood in Tension Based on Image Processing: Part 1. Tension Parallel- and Perpendicular-to-Grain and Comparisons with Isotropic Behaviour, *Silva Fennica,* Vol. 34, No. 3, 2000, pp. 251-259.
[9] S. Samarasinghe, G. D. Kulasiri, Displacement fields of wood in tension based on image processing: Part 2. Crack-tip displacements in mode-I and mixed-mode fracture, *Silva Fennica*, Vol. 34, No. 3, 2000, pp.261-274.
[10] H. Nowack, K.H. Trautmann, K. Schulte, G. Luetjering, *Sequence effects on fatigue crack propagation, Mechanical and Microstructural Contributions*, ASTM Special Technical Publication, 1979.
[11] J. Lankford, D.L. Davidson, K.S. Chan, The influence of crack tip plasticity in the growth of small fatigue cracks, *Metallurgical and Materials Transactions A-Physical Metallurgy and Materials Science*,Vol. 15, No.8,1984, pp. 1579-1588.
[12] J.P. Zhang, D. Venugopalan, Effects of notch radius and anisotropy on the crack tip plastic zone, *Engineering Fracture Mechanics*, Vol. 26, No. 6, 1987, pp. 913-925.
[13] G. Xin, W. Hangong, K. Xingwu, J. Liangzhou,

Analytic solutions to crack tip plastic zone under various loading conditions, *Eur J Mech A/Solids*, Vol. 29, No. 4, 2010, pp. 738-745.

[14] M.A. Sutton, W.J. Wolaters, W.H. Peters, W.F. Ranson, S.R. Mcneill, Determination of Displacements using an Improved Digital Correlation Method, *Image and Vision Computing*, Vol.1, No. 3, 1983, pp. 133-139.

[15] F. Hild, S. Roux, Digital image correlation: from displacement measurement to identification of elastic properties - a review, *Strain,* Vol.42, 2006, pp. 69-80.

[16] Zhao Jian, Zhao Dong, and Zhang Zhe, Assessment of Gradient-based Digital Speckle Correlation Measurement Errors, *Journal of the Optical Society of Korea*, Vol. 16, No. 4, 2012, pp. 372-380.

[17] G.C. Sih, P.C. Paris, G.R. Irwin, On cracks in rectilinearly anisotropic bodies, *International Journal of Fracture Mechanics*, Vol. 1, No. 3, 1965, pp 189-203.

[18] P.D. Shah, C.L. Tan, X. Wang, T-stress solutions for two-dimensional crack problems in anisotropic elasticity using the boundary element method, *Fatigue & Fracture of Engineering Materials & Structures*, Vol. 29, No.5, 2006, pp. 343-356.

[19] R. Hill, *Mathematical theory of plasticity*, Oxford University Press, 1950.

[20] G. J. Pataky, M.D. Sangid, H. Sehitoglu, et.al., Full field measurements of anisotropic stress intensity factor ranges in fatigue, *Engineering Fracture Mechanics*, Vol.94, 2012, pp. 13-28.

[21] David Grégoire, Hubert Maigre, Fabrice Morestin, New experimental techniques for dynamic crack localization, *European Journal of Computational Mechanics/Revue Européenne de Mécanique Numérique*, Vol. 18, No. 3-4, 2009, pp. 255-283.

[22] Wang Liyu, Lu Zhenyou, Twelve Elastic Constants of Betula platyphylla Suk., *Forestry Studies in China*, Vol. 6, No.1, 2004, pp. 37-41.

[23] H.W. Schreier, J.R. Braasch, M.A. Sutton, Systematic Errors in Digital Image Correlation caused by Intensity Interpolation, *Optical Engineering*, Vol. 39, No.11, 2000, pp. 2915-2921.